Geosci. Model Dev., 16, 5131–5151, 2023
https://doi.org/10.5194/gmd-16-5131-2023

Geoscientific Model Development
Open Access
EGU

Modernizing the open-source community Noah with multi-parameterization options (Noah-MP) land surface model (version 5.0) with enhanced modularity, interoperability, and applicability

Cenlin He[1], Prasanth Valayamkunnath[1,5], Michael Barlage[2], Fei Chen[1], David Gochis[1], Ryan Cabell[1], Tim Schneider[1], Roy Rasmussen[1], Guo-Yue Niu[3], Zong-Liang Yang[4], Dev Niyogi[4], and Michael Ek[1]

[1]National Center for Atmospheric Research (NCAR), Boulder, Colorado, USA
[2]NOAA Environmental Modeling Center (EMC), College Park, Maryland, USA
[3]Department of Hydrology and Atmospheric Sciences, University of Arizona, Tucson, Arizona, USA
[4]Department of Earth and Planetary Sciences, University of Texas Austin, Austin, Texas, USA
[5]Indian Institute of Science Education and Research, Thiruvananthapuram, India

Correspondence: Cenlin He (cenlinhe@ucar.edu)

Received: 5 April 2023 – Discussion started: 12 April 2023
Revised: 15 July 2023 – Accepted: 4 August 2023 – Published: 8 September 2023

Abstract. The widely used open-source community Noah with multi-parameterization options (Noah-MP) land surface model (LSM) is designed for applications ranging from uncoupled land surface hydrometeorological and ecohydrological process studies to coupled numerical weather prediction and decadal global or regional climate simulations. It has been used in many coupled community weather, climate, and hydrology models. In this study, we modernize and refactor the Noah-MP LSM by adopting modern Fortran code standards and data structures, which substantially enhance the model modularity, interoperability, and applicability. The modernized Noah-MP is released as the version 5.0 (v5.0), which has five key features: (1) enhanced modularization as a result of re-organizing model physics into individual process-level Fortran module files, (2) an enhanced data structure with new hierarchical data types and optimized variable declaration and initialization structures, (3) an enhanced code structure and calling workflow as a result of leveraging the new data structure and modularization, (4) enhanced (descriptive and self-explanatory) model variable naming standards, and (5) enhanced driver and interface structures to be coupled with the host weather, climate, and hydrology models. In addition, we create a comprehensive technical documentation of the Noah-MP v5.0 and a set of model benchmark and reference datasets. The Noah-MP v5.0 will be coupled to various weather, climate, and hydrology models in the future. Overall, the modernized Noah-MP allows a more efficient and convenient process for future model developments and applications.

1 Introduction

Land surface models (LSMs) are useful modeling tools for resolving terrestrial responses to and interactions with the atmosphere, ocean, glaciers, and sea ice in the earth system. Traditionally, LSMs were thought to mainly provide lower boundary conditions to the coupled atmospheric models. However, modern LSMs have been increasingly employed as indispensable components in the climate and weather systems to offer biogeophysical and biogeochemical insights for understanding and quantifying the impact and evolution of climate, weather, and the integrated earth environment (Blyth et al., 2021). LSMs have been widely applied to tackle many important societally relevant challenges, such as drought, flood, heat waves, water availability, agriculture, food security, wildfires, deforestation, and urbanization (Bonan and Doney, 2018).

Among many LSMs that have been developed in the past few decades, the open-source community Noah with multi-parameterization options (Noah-MP; Niu et al., 2011; Yang et al., 2011) is one of the most widely used state-of-the-art LSMs. The article describing the Noah-MP model by Niu et al. (2011) is de facto the most cited LSM paper of the last 10 years, highlighting its worldwide popular usage in the international science community. Compared to its predecessor, the Noah LSM (Chen et al., 1996, 1997; Chen and Dudhia, 2001; Ek et al., 2003), Noah-MP significantly improves upon the known Noah limitations by employing enhanced treatments of the vegetation canopy, snowpack, soil processes, groundwater, and their complex interactions, as well as through its additional capabilities for critical land processes (e.g., crop, irrigation, tile drainage, groundwater, urban, carbon, and nitrogen cycles). Another unique feature of Noah-MP is the inclusion of multiple physics options for different land processes, which allows for the multi-physics model ensemble experiments for uncertainty assessment and the testing of competing hypotheses (Zhang et al., 2016; J. Li et al., 2020).

Noah-MP can be applied to various spatial scales, spanning from point scale locally to ~ 100 km resolution globally, and temporal scales, spanning from sub-daily to decadal timescales. Since its original development, Noah-MP has been used in many important applications, including numerical weather prediction (Suzuki and Zupanski, 2018; Ju et al., 2022), high-resolution climate modeling (Gao et al., 2017; Liu et al., 2017; Rasmussen et al., 2023), land data assimilation (Kumar et al., 2019; Xu et al., 2021; Nie et al., 2022; Shu et al., 2022), drought (Arsenault et al., 2020; Niu et al., 2020; Wu et al., 2021; Abolafia-Rosenzweig et al., 2023a), wildfire (Kumar et al., 2021; Abolafia-Rosenzweig et al., 2022a, 2023b), snowpack evolution (Wrzesien et al., 2015; He et al., 2019; Jiang et al., 2020), hydrology and water resources (Cai et al., 2014; Liang et al., 2019; X. Y. Zhang et al., 2022; Hazra et al., 2023), crop and agricultural management (Liu et al., 2016; Ingwersen et al., 2018; Warrach-Sagi et al., 2022; Valayamkunnath et al., 2022; Zhang et al., 2020, 2023), urbanization and heat islands (Xu et al., 2018; Salamanca et al., 2018; Patel et al., 2022), biogeochemical cycles (Cai et al., 2016; Brunsell et al., 2021), wind erosion (Jiang et al., 2021), wetland (Z. Zhang et al., 2022), groundwater (Barlage et al., 2015, 2021; Li et al., 2022), and landslide hazard (Zhuo et al., 2019).

Currently, Noah-MP has been implemented into many community research and operational weather, climate, and hydrology models, including the Weather Research and Forecasting (WRF) model, the Model for Prediction Across Scales (MPAS), the NOAA operational National Water Model (NWM), the NOAA Unified Forecast System (UFS), the NASA Land Information System (LIS), and the NCAR High-Resolution Land Data Assimilation System (HRLDAS).

Despite its popular usage in the international research and application communities, the Noah-MP core code engine was designed 12 years ago and is outdated, and it does not take advantage of modern Fortran language architecture. It has a single lengthy ($> 12\,000$ lines) Fortran source file that lumps together all model physics with complex code and data structures using an inconsistent format, and it does not follow the modern Fortran 2003 code standard (https://j3-fortran.org/doc/year/04/04-007.pdf, last access: 4 September 2023). This makes the Noah-MP model code difficult for users and developers to read, modify, and test, as well as to implement and apply to other community models. Furthermore, a lengthy code is error prone and challenging to debug. These issues limit the further development and application of Noah-MP.

Therefore, this effort aims to modernize (refactor) the entire Noah-MP model by adopting modern Fortran 2003 code standards and data structures, which substantially enhance the model modularity, interoperability, and applicability. The base code used for refactoring is the Noah-MP version 4.5 (released in December 2022; https://github.com/NCAR/noahmp/tree/release-v4.5-WRF, last access: 4 September 2023), and the refactoring effort does not change the model physics. We release the modernized (refactored) Noah-MP as version 5.0 (v5.0; https://github.com/NCAR/noahmp, last access: 4 September 2023), which includes five key features: (1) enhanced modularization as a result of reorganizing model physics into individual process-level Fortran module files, (2) an enhanced data structure with new hierarchical data types and optimized variable declaration and initialization structures, (3) an enhanced code structure and subroutine calling workflow as a result of leveraging the new data structure and modularization and refining the code to be more concise, (4) an enhanced (descriptive and self-explanatory) model variable naming standard, and (5) an enhanced driver and interface code structures to couple with host weather, climate, and hydrology models. In addition, we have created a comprehensive technical documentation (He et al., 2023a) to describe the model physics and details of the refactored Noah-MP and a set of model benchmark and reference datasets for future comparison and assessment. Overall, the modernized open-source community Noah-MP model (version 5.0) will allow a more efficient and convenient process for future model developments and applications. The framework and practice in the course of refactoring the entire Noah-MP code is also applicable to other LSMs and Earth system models (ESMs).

This paper reports the key features of the modernized Noah-MP v5.0 and is organized as follows. Section 2 briefly summarizes the Noah-MP model physics, including several updates since its original development. Sections 3–7 introduce the key features of the modernized Noah-MP in terms of enhanced model modularization, data type, code structure, variable naming, and coupling structure in relation to host models. Section 8 describes the model benchmarking

and reference datasets. Section 9 provides the release information of the model code and the technical documentation. Section 10 concludes the paper with future model development plans.

2 Noah-MP version 5.0 model physics

2.1 Noah-MP description

Noah-MP (Niu et al., 2011) was originally developed based on the Noah LSM (Chen et al., 1996, 1997; Chen and Dudhia, 2001; Ek et al., 2003) to augment its modeling capabilities with enhanced physical representations and treatments of dynamic vegetation, canopy interception and radiative transfer processes, multi-layer snowpack physics, and soil and hydrological processes. The history of the model development and evolution has been described in the technical documentation (He et al., 2023a). Noah-MP is designed to simulate land surface and subsurface energy and water processes in both uncoupled and coupled modes with atmospheric or hydrological models at sub-daily timescales and high spatial resolutions (even for point scale). This further allows the use of Noah-MP in different hydrological, weather, and climate models for applications in a wide range of spatial and temporal scales with proper integration in time and space.

The Noah-MP land grid is divided into two sub-grid tiles, namely vegetated and non-vegetated grounds, based on vegetation cover fraction. The biogeophysical and biogeochemical processes are treated separately for the vegetated and bare grounds. A "big-leaf" canopy treatment is adopted, which is characterized by canopy properties dependent on vegetation types. Noah-MP accounts for a multiple-layer snowpack, where snow ice and liquid water content, density, depth, and temperature are simulated dynamically. There are also multilayer soil thermal and hydrological processes with dynamically evolving soil temperature and water content. The vegetation, snow, and soil components in Noah-MP are closely coupled and interact with each other via complex energy, water, and biochemical processes. Their detailed physical formulations and parameterizations in Noah-MP v5.0 are described in the technical documentation (He et al., 2023a). Below, we briefly summarize the energy, water, and biochemical processes in Noah-MP v5.0.

2.2 Noah-MP energy processes

Noah-MP resolves energy budgets and processes separately for vegetated and non-vegetated ground portions of each grid (Niu et al., 2011). The vegetation cover fraction, either from observational inputs or model calculations based on leaf area index (LAI) inputs or predicted by the dynamic vegetation module, is used to separate vegetated and bare grounds. The grid-mean energy states and fluxes are calculated as an average of vegetated- and bare-ground values weighted by vegetation cover fraction. For surface radiative processes driven by incoming shortwave and longwave radiation (atmospheric forcing), Noah-MP simulates the radiative absorption and scattering by the canopy and ground (soil or snow), as well as the longwave emissions by the canopy and ground (soil or snow). The net absorbed total (shortwave and longwave) radiative flux is balanced by precipitation-advected heat flux, total surface sensible and latent heat fluxes, and ground heat flux. The precipitation-advected heat flux represents the heat flux advected from precipitation (rain or snow) to the canopy or ground due to the temperature difference between precipitation (surface air) and the canopy or ground. The total surface sensible heat includes the sensible heat from the canopy, snowpack, and soil surfaces. The total surface latent heat includes the latent heat from snowpack sublimation, soil evaporation, canopy snow sublimation, canopy water evaporation, and plant transpiration. The ground heat flux is the heat flux leaving the ground surface to drive the subsurface snow or soil phase change and/or temperature changes.

To model the aforementioned surface energy flux components, Noah-MP dynamically calculates a number of key land surface properties, including ground snow cover fraction, surface roughness, canopy and ground thermal properties, snow and soil albedo, surface emissivity, and canopy radiative transfer. Many of these property and process calculations have multiple physics options (see Sect. 2.6). Based on the canopy and ground energy balance, Noah-MP further solves the temperature and phase change for the canopy, snowpack, and soil. Figure 1 summarizes the key energy processes and budget components, as well as the energy balance equation, in Noah-MP v5.0. Note that the energy processes in glacier grids are treated similarly to those in 100 % bare (non-vegetated)-ground grids, except for the fact that the soil is replaced by glacier ice with ice-specific properties.

2.3 Noah-MP water processes

Noah-MP accounts for five major water budget components, including precipitation, evapotranspiration (ET), total runoff, net lateral flow, and total water storage change intercepted by the canopy and in snow, soil, and aquifers. For precipitation, Noah-MP has several temperature-based rainfall–snowfall partitioning parameterizations, or it can use the partitioning from atmospheric models directly (see Sect. 2.6). Noah-MP simulates the canopy interception and throughfall of rain and snow, where the intercepted rain and snow on the canopy can go through unloading or dripping, frost, sublimation, melting, and freezing processes. Net evaporation loss from the canopy-intercepted liquid water (evaporation minus dew), net sublimation from the canopy-intercepted snow (sublimation minus frost), transpiration (via plant hydraulics), net soil surface evaporation, and net snowpack sublimation together contribute to the total surface ET. Noah-MP dynamically simulates multi-layer snowpack water storage (ice and liquid water) changes driven by snowfall or rainfall, frost, sublimation, freezing, and melting. The snowmelt water out

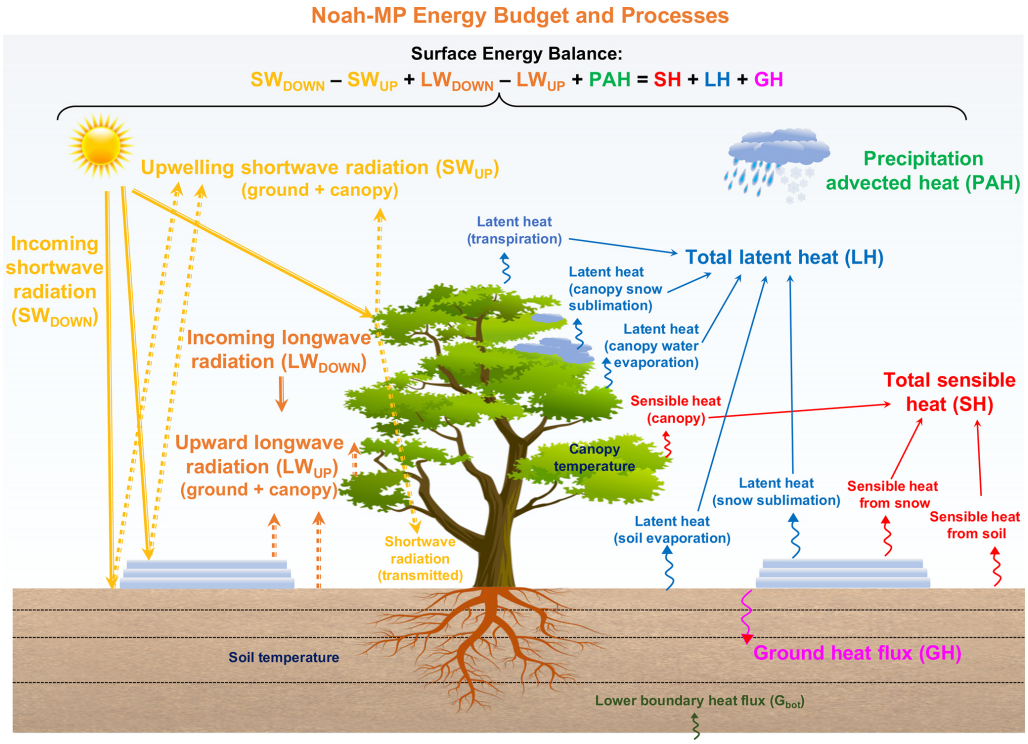

Figure 1. Schematic diagram of energy budget and processes represented in Noah-MP version 5.0.

of snowpack and the rainfall at the soil surface are further partitioned into surface runoff and infiltration based on multiple runoff and infiltration physics options (see Sect. 2.6). Soil moisture and unsaturated water flow across soil layers are simulated using the one-dimensional Richards equation. Two optional groundwater schemes, one without 2-D lateral flow (Niu et al., 2007) and one with 2-D lateral flow (Fan et al., 2007; Miguez-Macho et al., 2007), are available in Noah-MP to simulate groundwater dynamics, including groundwater recharge, water table change, baseflow, seepage, and/or lateral flow. Noah-MP also includes dynamic irrigation and tile drainage processes for agricultural management applications (Valayamkunnath et al., 2021, 2022). Figure 2 summarizes the key water processes and budget components, as well as the water balance equation, in Noah-MP v5.0. Note that the water processes in glacier grids are treated similarly to those in 100 % bare-ground grids, except for the fact that all the soil and subsurface hydrological processes are removed and replaced by glacier ice (He et al., 2023a).

2.4 Noah-MP biochemical processes

Currently, the community version of Noah-MP only accounts for carbon processes for biochemical cycles, while nitrogen dynamics and soil carbon dynamics have been developed in non-community Noah-MP versions managed by individual research groups (e.g., Cai et al., 2016; X. Zhang et al., 2022). We will synthesize and integrate individual Noah-MP updates into the community version in the future (see Sect. 2.5 for more discussions). Noah-MP simulates carbon processes for both natural and/or generic vegetation (Niu et al., 2011) and explicit agricultural crops (Liu et al., 2016). The carbon processes related to vegetation growth dynamics include (1) carbon assimilation from photosynthesis by shaded and sunlit leaves, (2) carbon allocation to different parts of vegetation (leaf, stem, wood, and root) and soil carbon pools (fast and slow carbon), (3) carbon loss due to respiration of different vegetation and soil carbon pools, (4) carbon transfer between vegetation and fast soil carbon pools through vegetation (leaf, stem, wood, and root) turnover and seasonal death of leaves and stems, and (5) soil carbon pool conversion through soil carbon stabilization. The total carbon flux to the atmosphere and the net primary productivity are computed based on the aforementioned carbon processes. Figure 3 summarizes the key carbon processes and budget components, as well as the carbon balance equation, in Noah-MP v5.0. Note that the carbon processes for crop growth are treated similarly to those for natural vegetation, except for the fact that the wood component of plants is removed, and the grain component of crops is added with additional carbon conversion from the leaf, stem, and root to grain, depending on the crop-growing stages.

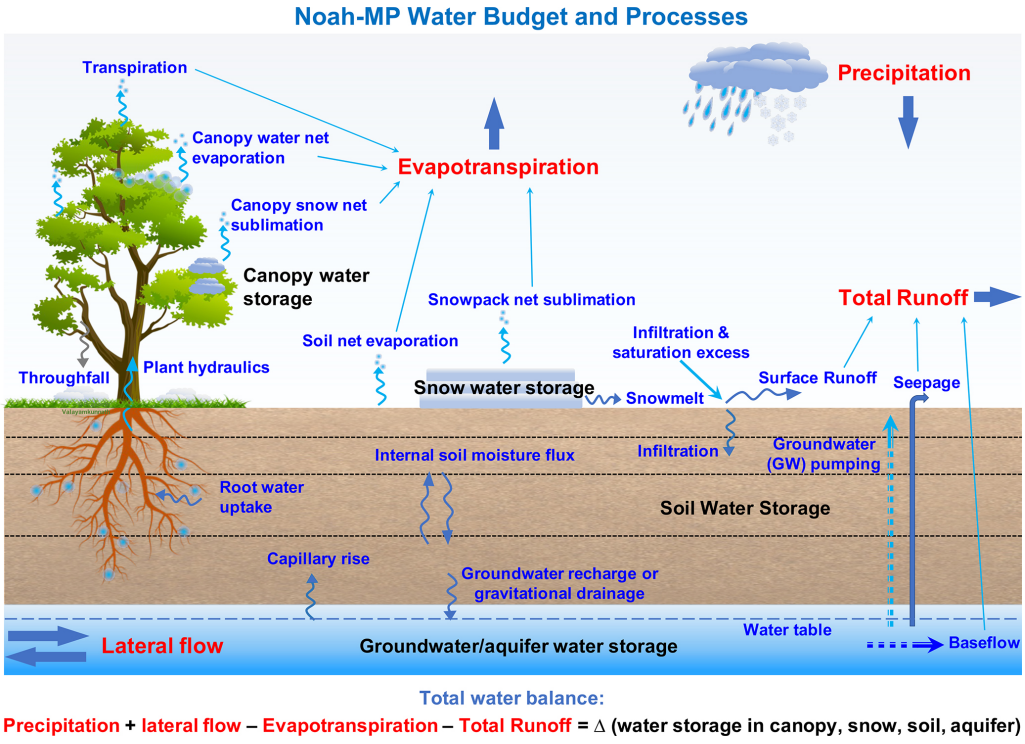

Figure 2. Schematic diagram of water budget and processes represented in Noah-MP version 5.0.

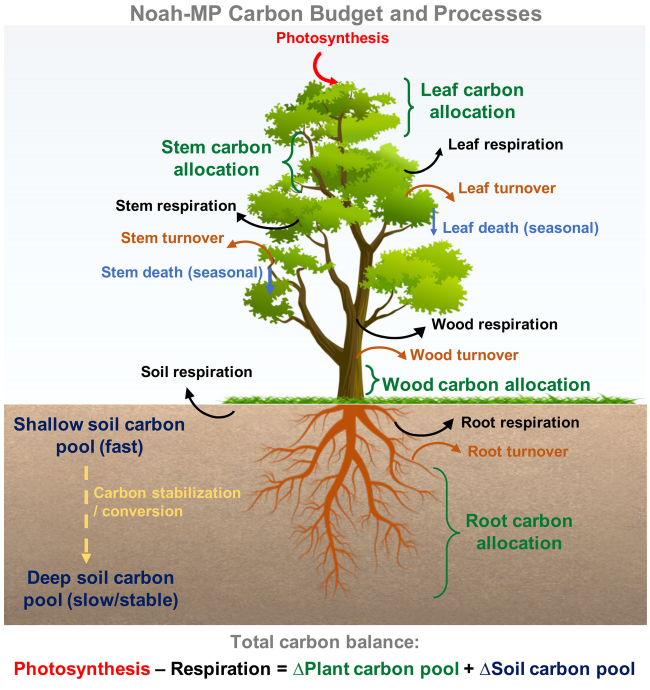

Figure 3. Schematic diagram of carbon budget and processes represented in Noah-MP version 5.0.

2.5 Noah-MP physics updates since original development

Since the release of the original Noah-MP in the year 2011 (Niu et al., 2011), there have been several important updates in Noah-MP physics. Some of the updates have been included in the community version of Noah-MP v5.0, while some are only available in the non-community versions managed by individual research groups. We will make efforts to synthesize and integrate individual Noah-MP updates into the community version in the future by working with those developer teams. Here, to the best of our knowledge, we briefly list the major Noah-MP physics updates from the community in the past decade.

The new or enhanced physics included in the community Noah-MP version 5.0 since 2011 are as follows: (1) the Miguez-Macho–Fan (MMF) groundwater scheme (Barlage et al., 2015); (2) three additional runoff schemes, namely the variable infiltration capacity (VIC), dynamic VIC, and Xinanjiang schemes (McDaniel et al., 2020); (3) tile drainage schemes (Valayamkunnath et al., 2022); (4) dynamic irrigation schemes (sprinkler, micro-, and flooding irrigation) (Valayamkunnath et al., 2021); (5) a dynamic crop growth model for corn and soybeans (Liu et al., 2016) with enhanced C3 and C4 crop parameters (Zhang et al., 2020); (6) coupling with urban canopy models (Xu et al., 2018; Salamanca et al., 2018) with local-climate-zone modeling capabilities (Zonato et al., 2021); (7) enhanced snow cover, snow compaction,

and wind canopy absorption parameters (He et al., 2021); and (8) a wet-bulb temperature-based snow–rain partitioning scheme (Wang et al., 2019).

The new (enhanced) physics currently not included in the community Noah-MP version 5.0 since 2011 are as follows: (1) nitrogen dynamics (Cai et al., 2016), (2) big-tree plant hydraulics (Li et al., 2021), (3) dynamic root optimization (Wang et al., 2018) with an explicit representation of plant water storage (Niu et al., 2020), (4) additional snow cover parameterizations (Jiang et al., 2020), (5) coupling with a wind erosion model (Jiang et al., 2021), (6) wetland representation and dynamics (Z. Zhang et al., 2022), (7) a unified turbulence parameterization throughout the canopy and roughness sublayer (Abolafia-Rosenzweig et al., 2021), (8) enhanced snow albedo representations (Abolafia-Rosenzweig et al., 2022b), (9) coupling with a snow radiative transfer (SNICAR) model (Wang et al., 2020, 2022), (10) an organic soil layer representation on forest floors (Chen et al., 2016) and a microbial-explicit soil organic carbon decomposition model (MESDM; X. Zhang et al., 2022), (11) coupling with atmospheric dry deposition of air pollutants (Chang et al., 2022), (12) enhanced permafrost soil representations (X. Li et al., 2020); (13) spring wheat crop dynamics (Zhang et al., 2023), (14) new treatment of thermal roughness length (Chen and Zhang, 2009), (15) the GECROS crop model (Ingwersen et al., 2018; Warrach-Sagi et al., 2022), and (16) a 1-D dual-permeability flow model (based on the mixed-form Richards equation) representing preferential flow through variably saturated soil with surface ponding being developed at the University of Arizona.

2.6 Noah-MP multi-physics options

One unique feature and advantage of Noah-MP is the inclusion of multiple physics options for different land processes for testing competing hypotheses (i.e., options) and multi-model ensemble simulations. Table 1 summarizes all the available physics options in the community Noah-MP v5.0. In particular, compared to previous Noah-MP versions, we have separated the runoff options for surface and subsurface runoff processes, and added a new physics option for snow thermal conductivity calculations, which were originally hard-coded without the namelist control capability. More detailed descriptions of each physics option are provided in the technical documentation (He et al., 2023a).

3 Enhanced model modularization in Noah-MP version 5.0

In the Noah-MP v5.0, we have modularized all model physics by separating and re-organizing each code subroutine into individual process-level Fortran module files with new descriptive, self-explanatory module and subroutine names. As such, each model physics item or scheme has its own separate module. Figure 4 shows the calling tree of the modularized Noah-MP main model physics workflow. Figures 5–7 show the calling tree of the modularized energy, water, and carbon processes, respectively. Compared to the previous Noah-MP versions that have a single, lengthy source file lumping together all model subroutines with non-self-explanatory names, the highly modularized model structure of the Noah-MP v5.0 provides a much clearer, neater, and more organized way for users and developers to understand and follow the model logic and physics. These new modules use consistent coding formats and standards, offering convenience for code reading, writing, and debugging. The highly modularized model structure facilitates future development by allowing specific model physics to be worked on in isolation or replaced without interfering with other parts of the model code. This modularization also allows external community weather, climate, and hydrology models to easily adopt specific Noah-MP physical processes or schemes as independent process-level module files and to implement them for testing and coupling.

4 Enhanced data structure in Noah-MP version 5.0

In the Noah-MP v5.0, we have enhanced the data structure with new hierarchical data types, which allows for a more efficient and convenient control of model variables and substantially simplifies the code structures and calling interface (Sect. 5). Figure 8 summarizes the new Noah-MP data type hierarchy and gives some examples of model variable expression based on the hierarchical data types. Specifically, we have defined an overarching "noahmp" main data type, which includes "forcing" for the atmospheric-forcing variable type; "config" for the model configuration variable type, with "domain" and "namelist" subtypes; "energy" for the energy-related variable type; "water" for the water-related variable type; and "biochem" for the biochemistry-related variable type. The energy, water, and biochem types are further divided into "flux", "state", and "param" subtypes for flux, state, and parameter variables. This hierarchical data structure provides a better organization and management of model variables and their physical attributes. We have also optimized the variable declaration and initialization structures based on those new data types and a consistent coding format and standard. In addition, we have re-defined many key local model state, flux, and parameter variables in the base code to be global variables in the refactored code, which allows for better tracking and management of these variables for diagnosis, transference between Noah-MP and host models, and coupling with data assimilation systems.

5 Enhanced code structure in Noah-MP version 5.0

Leveraging the model modularization (Sect. 3) and new data types (Sect. 4) in the Noah-MP v5.0, we have further refined

Table 1. List of Noah-MP version 5.0 multi-physics options.

Noah-MP physics	Option	Notes (* indicates the default option)
OptDynamicVeg Options for dynamic (prognostic) vegetation	1	Off (use table LeafAreaIndex; use VegFrac = VegFracGreen from input) (Niu et al., 2011; Yang et al., 2011)
	2	On (together with OptStomataResistance = 1) (Dickinson et al., 1998; Niu and Yang, 2004)
	3	Off (use table LeafAreaIndex; calculate VegFrac)
	4*	Off (use table LeafAreaIndex; use maximum vegetation fraction)
	5	On (use maximum vegetation fraction)
	6	On (use VegFrac = VegFracGreen from input)
	7	Off (use input LeafAreaIndex; use VegFrac = VegFracGreen from input)
	8	Off (use input LeafAreaIndex; calculate VegFrac)
	9	Off (use input LeafAreaIndex; use maximum vegetation fraction)
OptRainSnowPartition Options for partitioning precipitation into rainfall & snowfall	1*	Jordan (1991) scheme
	2	BATS (Biosphere–Atmosphere Transfer Scheme): when TemperatureAirRefHeight < freezing point + 2.2 (Yang and Dickinson, 1996)
	3	TemperatureAirRefHeight < freezing point (Niu et al., 2011)
	4	Use WRF microphysics output (Barlage et al., 2015)
	5	Use wet-bulb temperature (Wang et al., 2019)
OptSoilWaterTranspiration Options for soil moisture factor for stomatal resistance & ET	1*	Noah (soil moisture) (Ek et al., 2003)
	2	CLM (matric potential) (Oleson et al., 2004)
	3	SSiB (matric potential) (Xue et al., 1991)
OptGroundResistanceEvap Options for ground resistance to evaporation and/or sublimation	1*	Sakaguchi and Zeng (2009) scheme
	2	Sellers et al. (1992) scheme
	3	Adjusted Sellers et al. (1992) for wet soil
	4	Sakaguchi and Zeng (2009) for non-snow; rsurf = rsurf_snow for snow (set in NoahmpTable.TBL)
OptSurfaceDrag Options for surface layer drag and/or exchange coefficient	1*	Monin–Obukhov (M–O) similarity theory (Brutsaert, 1982)
	2	Original Noah (Chen et al., 1997)
OptStomataResistance Options for canopy stomatal resistance	1*	Ball–Berry scheme (Ball et al., 1987; Bonan, 1996)
	2	Jarvis scheme (Jarvis, 1976)
OptSnowAlbedo Options for ground snow surface albedo	1*	BATS snow albedo (Dickinson et al., 1993)
	2	CLASS snow albedo (Verseghy, 1991)
OptCanopyRadiationTransfer Options for canopy radiation transfer	1	Modified two-stream (gap = f (solar angle, 3D structure, etc.) < 1-VegFrac) (Niu and Yang, 2004)
	2	Two-stream applied to grid cell (gap = 0) (Niu et al., 2011)
	3*	Two-stream applied to vegetated fraction (gap = 1-VegFrac) (Dickinson, 1983; Sellers, 1985)

Table 1. Continued.

Noah-MP Physics	Option	Notes (* indicates the default option)
OptSnowSoilTempTime Options for snow or soil temperature time scheme (only layer 1)	1*	Semi-implicit; flux top boundary condition (Niu et al., 2011)
	2	Fully implicit (original Noah); temperature top boundary condition (Ek et al., 2003)
	3	Same as 1 but snow cover for skin temperature calculation (Niu et al., 2011)
OptSnowThermConduct Options for snow thermal conductivity	1*	Stieglitz scheme (Yen, 1965)
	2	Anderson (1976) scheme
	3	Constant (Niu et al., 2011)
	4	Verseghy (1991) scheme
	5	Douvill scheme (Yen, 1981)
OptSoilTemperatureBottom Options for lower boundary condition of soil temperature	1	Zero heat flux from bottom (DepthSoilTempBottom and TemperatureSoilBottom not used) (Niu et al., 2011)
	2*	TemperatureSoilBottom at DepthSoilTempBottom (8 m) read from a file (original Noah) (Ek et al., 2003)
OptSoilSupercoolWater Options for soil supercooled liquid water	1*	No iteration (Niu and Yang, 2006)
	2	Koren's iteration (Koren et al., 1999)
OptRunoffSurface Options for surface runoff	1	TOPMODEL with groundwater (Niu et al., 2007)
	2	TOPMODEL with an equilibrium water table (Niu et al., 2005)
	3*	Schaake scheme (original Noah) (Schaake et al., 1996)
	4	BATS surface and subsurface runoff (Yang and Dickinson, 1996)
	5	Miguez-Macho–Fan (MMF) groundwater scheme (Fan et al., 2007; Miguez-Macho et al., 2007)
	6	Variable infiltration capacity model surface runoff scheme (Liang et al., 1994)
	7	Xinanjiang infiltration and surface runoff scheme (Jayawardena and Zhou, 2000)
	8	Dynamic VIC surface runoff scheme (Liang and Xie, 2003)
OptRunoffSubsurface options for drainage & subsurface runoff	1–8	Similar to runoff option, separated from original Noah-MP runoff option, and currently tested and recommended the same option as surface runoff (default)
OptSoilPermeabilityFrozen Options for frozen soil permeability	1*	Linear effects, more permeable (Niu and Yang, 2006)
	2	Nonlinear effects, less permeable (Koren et al., 1999)
OptDynVicInfiltration Options for infiltration in dynamic VIC runoff scheme	1*	Philip scheme (Liang and Xie, 2003)
	2	Green–Ampt scheme (Liang and Xie, 2003)
	3	Smith–Parlange scheme (Liang and Xie, 2003)
OptTileDrainage Options for tile drainage Currently only tested and calibrated to work with runoff option = 3	0*	No tile drainage
	1	On (simple scheme) (Valayamkunnath et al., 2022)
	2	On (Hooghoudt's scheme) (Valayamkunnath et al., 2022)

Table 1. Continued.

Noah-MP physics	Option	Notes (* indicates the default option)
OptIrrigation Options for irrigation	0*	No irrigation
	1	Irrigation on (Valayamkunnath et al., 2021)
	2	Irrigation trigger based on crop season planting and harvesting dates (Valayamkunnath et al., 2021)
	3	Irrigation trigger based on LeafAreaIndex threshold (Valayamkunnath et al., 2021)
OptIrrigationMethod Options for irrigation method – only works when OptIrrigation > 0	0*	Method based on geo_em fractions
	1	Sprinkler method (Valayamkunnath et al., 2021)
	2	Micro- or drip irrigation (Valayamkunnath et al., 2021)
	3	Surface flooding (Valayamkunnath et al., 2021)
OptCropModel Options for crop model	0*	No crop model
	1	Liu et al. (2016) crop scheme
OptSoilProperty Options for defining soil properties	1*	Use input dominant soil texture
	2	Use input soil texture that varies with depth
	3	Use soil composition (sand, clay, organics) and pedotransfer function
	4	Use input soil properties
OptPedotransfer Options for pedotransfer functions – only works when OptSoilProperty = 3	1*	Saxton and Rawls (2006) scheme
OptGlacierTreatment Options for glacier treatment	1*	Include phase change of glacier ice
	2	Glacier ice treatment more like original Noah

the code structure and subroutine interface. A graphical representation of the refactored Noah-MP subroutine interface is depicted in Fig. 9. Specifically, the refined subroutine interface only requires passing the noahmp data type instead of each individual variable name because all relevant variables are defined and included in the noahmp data type. This significantly simplifies the code structure with much more concise and neat subroutine calls. The refined subroutine interface also makes future model development and code changes simpler, more efficient, and less error prone. For instance, if users want to add or remove a variable for a specific physical scheme, they only need to edit as few as three module files: variable type definition module, variable initialization module, the target physical scheme module, and if needed, the variable input and output module. There is no need to go through and change all the subroutine calls and interfaces that use the target variable.

6 Enhanced variable naming in Noah-MP version 5.0

In the Noah-MP v5.0, we have also renamed all the model variables using a more descriptive and self-explanatory naming standard, which clarifies the physical meaning of variables directly by their names and hence substantially lowers the hurdles of reading and understanding the code and model physics. The original variable names in the previous Noah-MP versions are hard to understand, in which case users have to repeatedly check the variables' definitions to know their physical meanings. For instance, the original variable name for canopy-intercepted total water is "CMC", while the new name is "CanopyTotalWater". Table 2 gives more examples of the enhanced variable naming in Noah-MP v5.0. A detailed Noah-MP variable glossary listing variables' original and new names, physical meanings, data types, and units is provided in the technical documentation (He et al., 2023) and the community Noah-MP GitHub repository.

7 Enhanced coupling structure with host models in Noah-MP version 5.0

We have further updated the Noah-MP driver and interface coupled with potential host weather, climate, and hydrology models. Figure 10 summarizes the interface and coupling structures in the Noah-MP v5.0. Specifically, the coupling

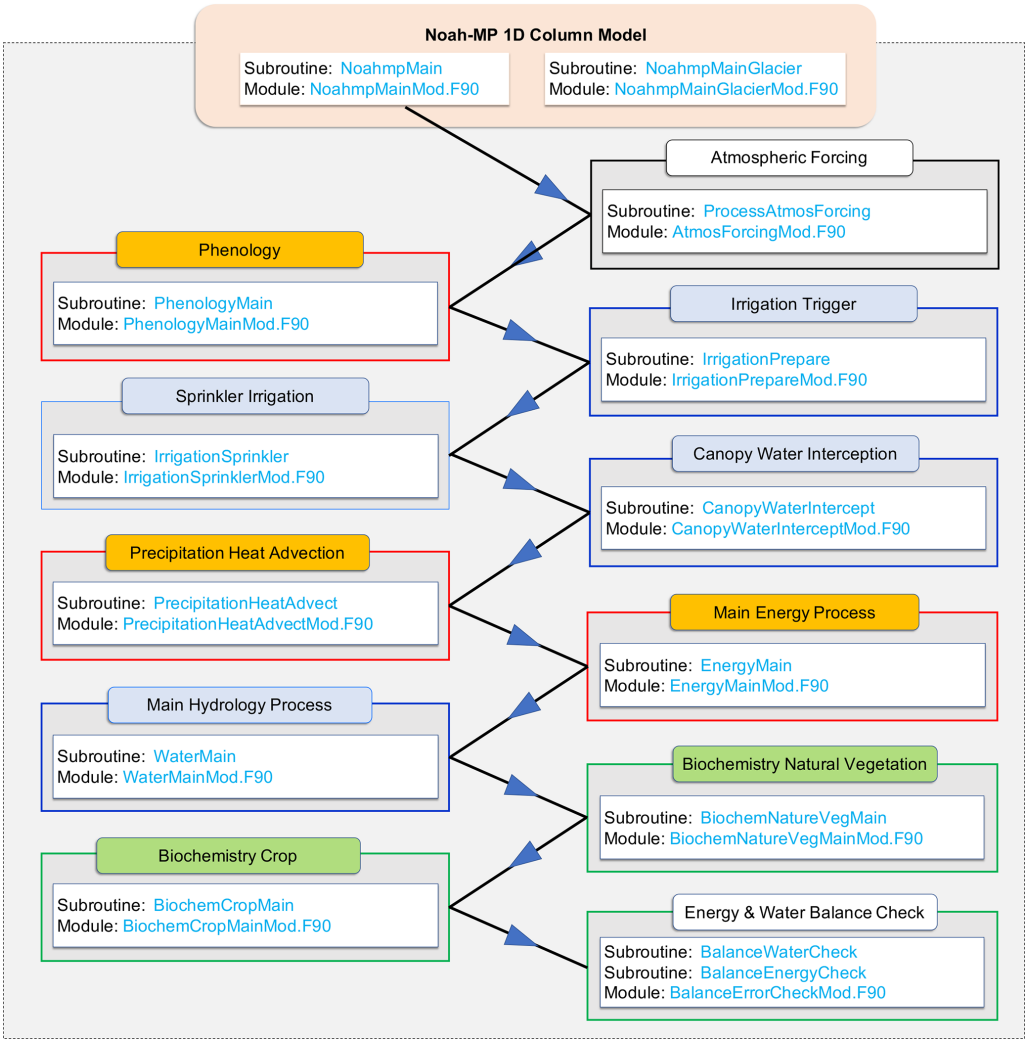

Figure 4. The modularized Noah-MP main physics calling tree in version 5.0. Blue boxes indicate water processes, orange boxes indicate energy processes, and green boxes indicate biochemical processes. The directions of the arrows indicate the process calling sequences and information flows. Note that the 1-D glacier column model has similar structures as the main non-glacier model, except for the fact that the vegetation-related processes are removed, and soil is replaced by glacier ice.

Table 2. Examples of new variable names based on a more descriptive and self-explanatory naming standard in the Noah-MP version 5.0 compared with the original names.

Variable physical meaning or definition	New name	Original name	Variable Type	Unit
Wetted or snowed fraction of canopy	CanopyWetFrac	FWET	Real	–
Canopy-intercepted liquid water	CanopyLiqWater	CANLIQ	Real	mm
Canopy-intercepted ice	CanopyIce	CANICE	Real	mm
Canopy-intercepted total water	CanopyTotalWater	CMC	Real	mm
Canopy capacity for snow interception	CanopyIceMax	MAXSNO	Real	mm
Canopy capacity for liquid water interception	CanopyLiqWaterMax	MAXLIQ	Real	mm
Ice fraction in snow layers	SnowIceFrac	FICE_SNOW	Real	–
Bulk density of snowfall	SnowfallDensity	BDFALL	Real	$kg\,m^{-3}$
Snow cover fraction	SnowCoverFrac	FSNO	Real	–
Snow layer ice	SnowIce	SNICE	Real	mm
Snow layer liquid water	SnowLiqWater	SNLIQ	Real	mm

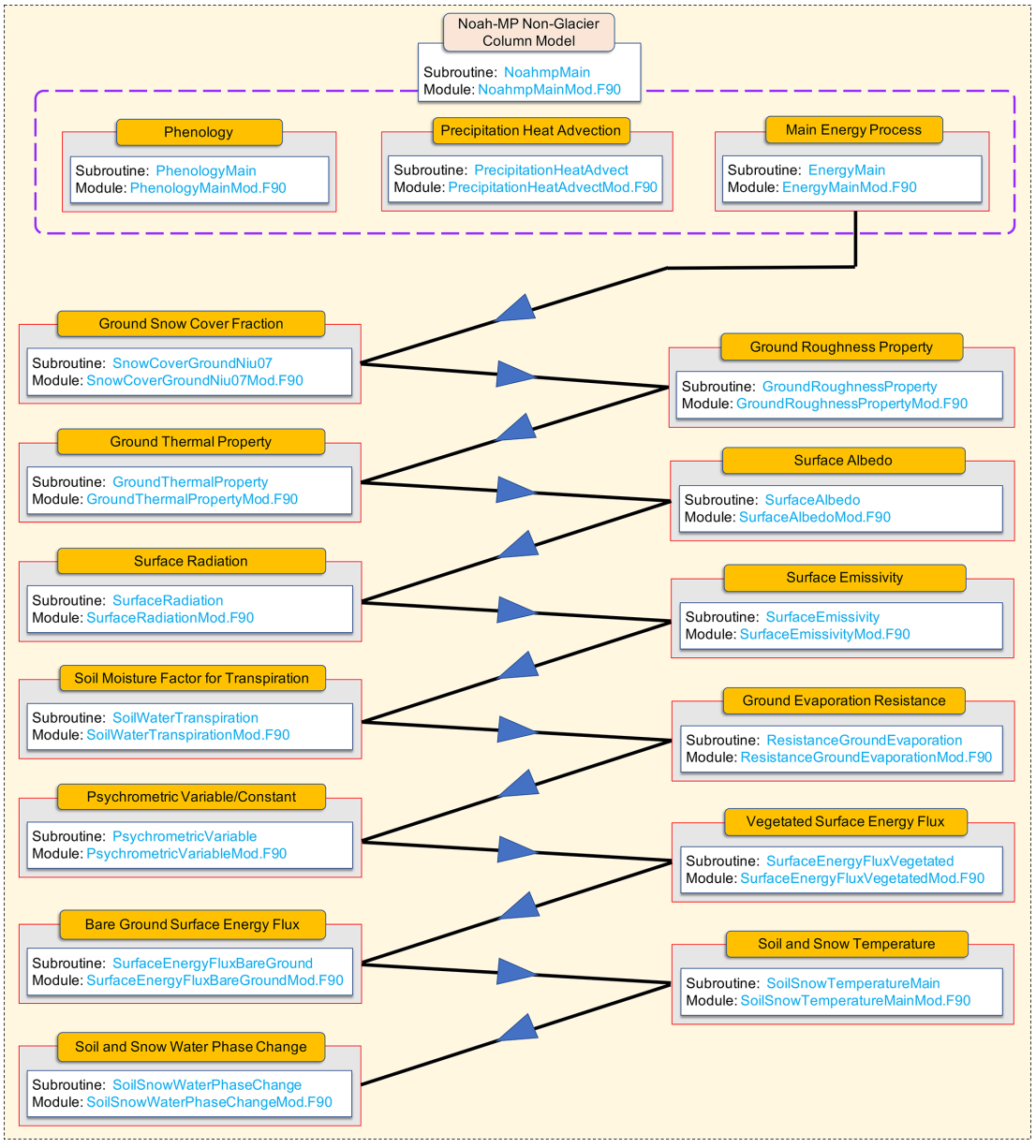

Figure 5. The modularized Noah-MP energy process calling tree in version 5.0. Note that the glacier model has similar structures, except for the fact that the vegetation-related processes are removed, and soil is replaced by glacier ice.

interface includes the following: (1) the definition of a 2-D (for structured grid mesh) or vectorized (for unstructured grid mesh) Noah-MP input–output data type, "NoahmpIO", to facilitate the input–output communication between host models and the core Noah-MP 1-D column model (noahmp data type); (2) the initialization of the NoahmpIO variables with values from host models; and (3) the main Noah-MP driver that calls the core 1-D column model and transfers between the NoahmpIO and noahmp variables as part of input–output processes. Currently, the coupling of the Noah-MP v5.0 with the NCAR/HRLDAS system has been successfully completed. The coupling of Noah-MP v5.0 with the NASA/LIS system and the WRF-Hydro/NWM system is ongoing. We also plan to couple the Noah-MP v5.0 with other host models in the future (Sect. 9), such as WRF, MPAS, and NOAA/UFS. Because of the enhanced coupling interface and structure in Noah-MP v5.0, we will only need to slightly adapt the coupling interface and driver to allow it to work with different host models. We will manage and maintain the interface and driver code for each host model in the community Noah-MP GitHub repository to ensure the compatibility between host models and updated core Noah-MP source code in the future, which will allow the smooth tran-

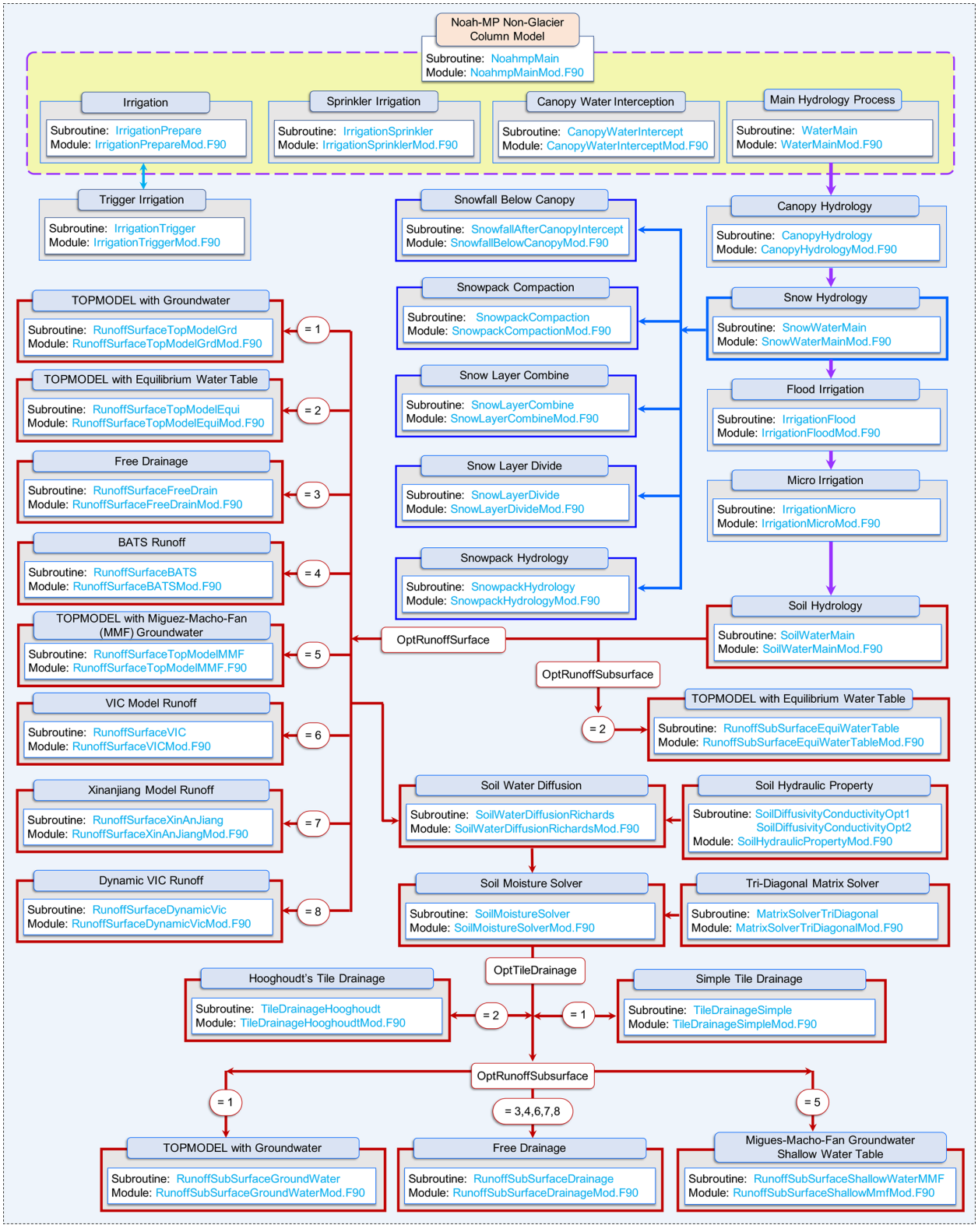

Figure 6. The modularized Noah-MP water process calling tree in version 5.0. Note that the glacier model has similar structures, except for the fact that it only includes the snowpack processes, and soil is replaced by glacier ice.

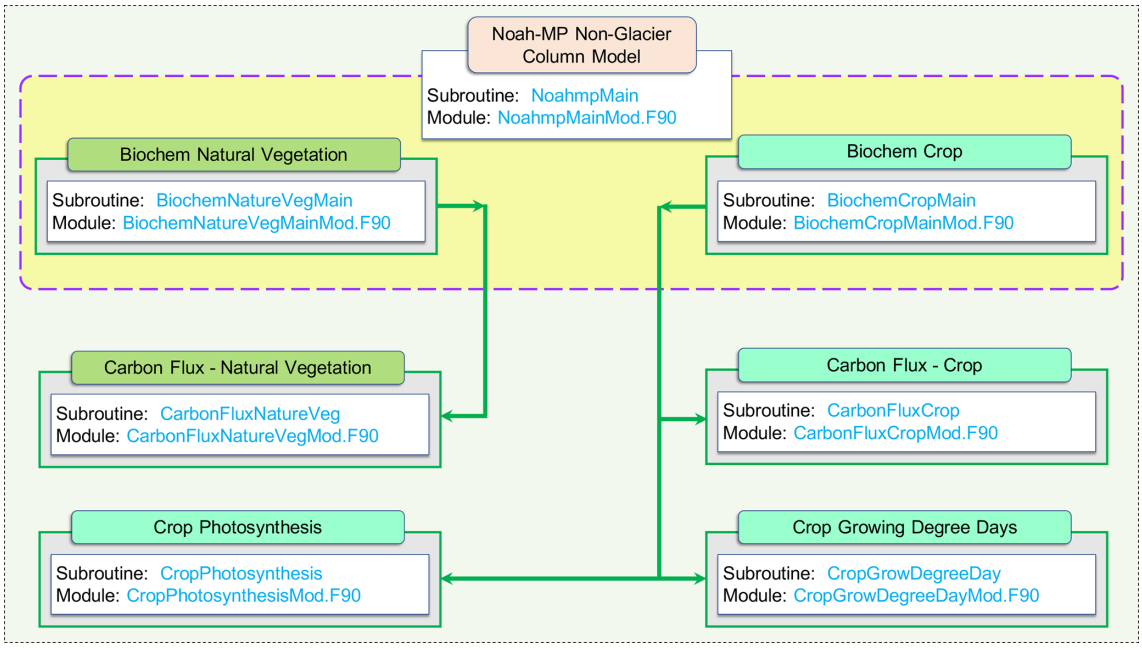

Figure 7. The modularized Noah-MP biochemical process calling tree in version 5.0. Note that, currently, the Noah-MP v5.0 only includes carbon processes. Note that the CropPhotosynthesis module is not used currently to avoid inconsistency with the photosynthesis calculations from the canopy stomatal resistance module.

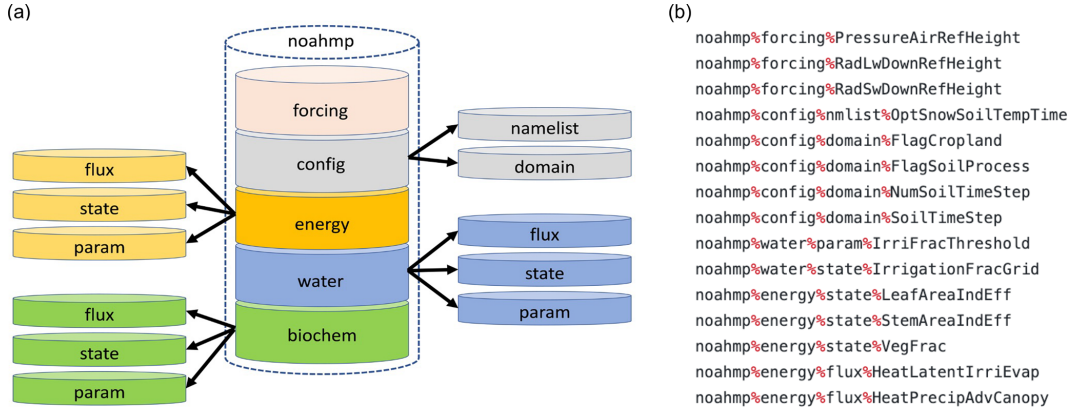

Figure 8. **(a)** The new hierarchical noahmp data types in the Noah-MP version 5.0. **(b)** Examples of model variable expression using the hierarchical data types.

sition and seamless synthesizing of Noah-MP updates in host models.

8 Benchmarking for Noah-MP version 5.0

To benchmark the functionality, reproducibility, and computational efficiency of the modernized Noah-MP code, we conducted a series of hierarchical test simulations during the course of the Noah-MP refactoring. Specifically, after refactoring each major Noah-MP model component or physics item (e.g., water, energy, carbon) listed in Fig. 4, we built simple driver modules to conduct benchmark simulations using each of these model component or physics items to test and ensure the bit-for-bit consistency between the refactored code and the base code for all Noah-MP physics options. Here is an example for the refactored Noah-MP water component model we built for benchmarking during the course of refactoring: https://github.com/cenlinhe/NoahMP_refactor/tree/water_refactor (last access: 4 September 2023), which was used to test the bit-for-bit consistency between the refactored and base Noah-MP water component codes.

After we completed the entire model refactoring, we conducted another set of test simulations using the completed Noah-MP v5.0 to ensure its bit-for-bit consistency with the

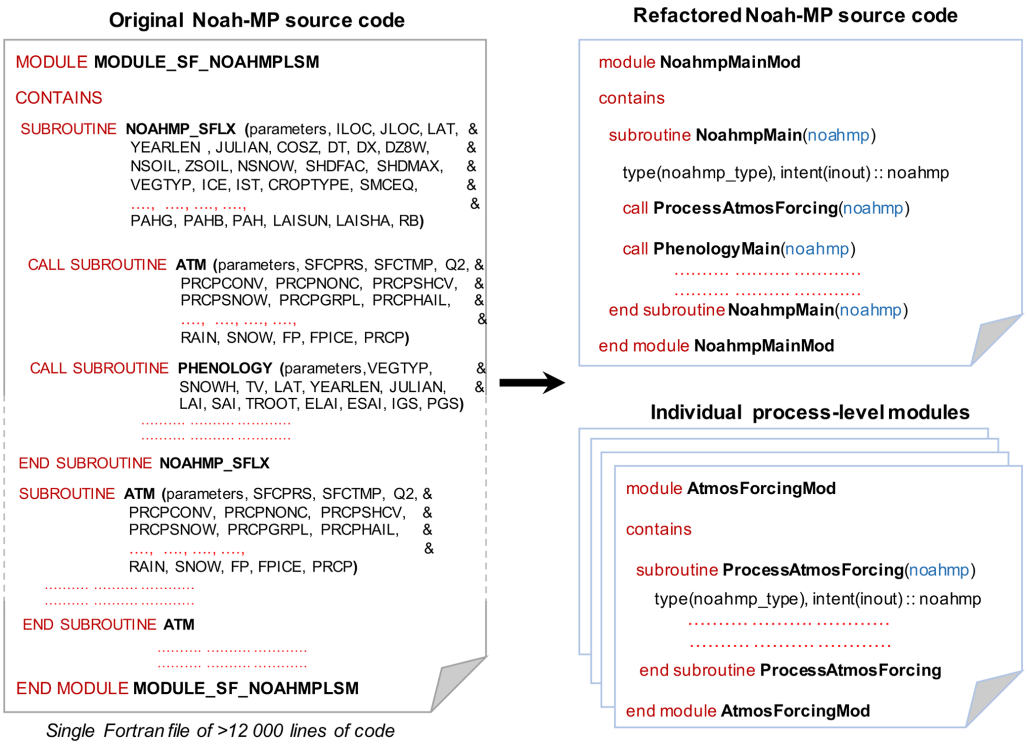

Figure 9. Demonstration of refactored subroutine interface and code structure in the Noah-MP version 5.0.

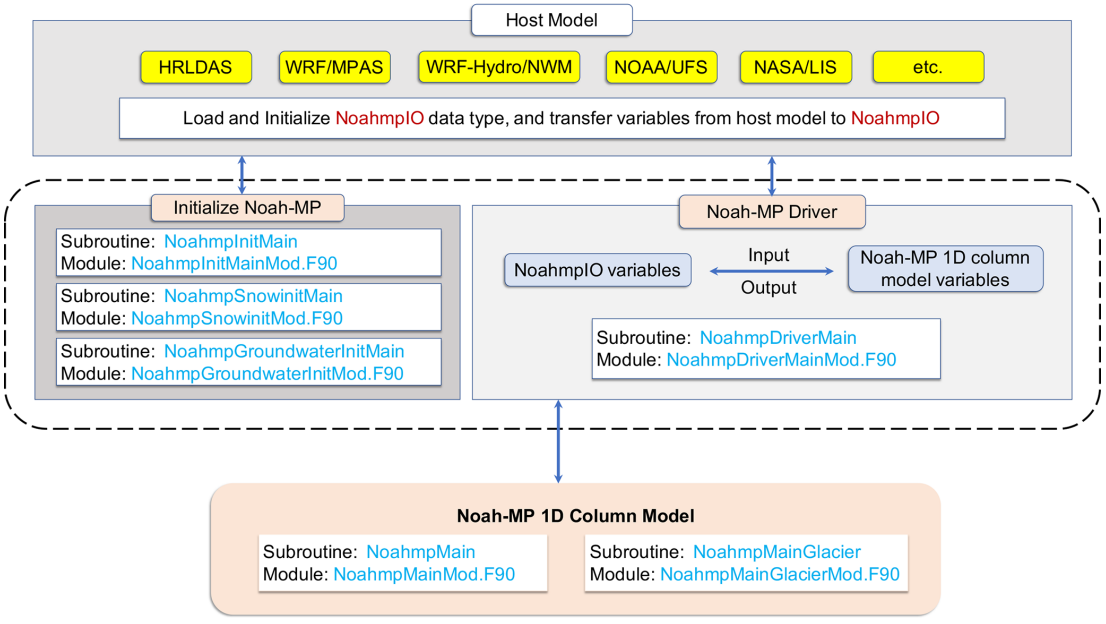

Figure 10. Workflow of the Noah-MP v5.0 driver and interface structures to couple with various host weather, climate, and hydrology models.

base model code for all different combinations of physics options, as well as to benchmark its computational efficiency. These tests were conducted via 1-year point-scale SNOTEL (Snow Telemetry) site 804 simulations, 1-year 12 km gridded continental US simulations, and 1-year 1 km gridded simulations over the central US agricultural regions (particularly to test individual physics options and combinations of physics options related to crops, irrigation, tile drainage, and groundwater). The tests all showed exactly the same results between

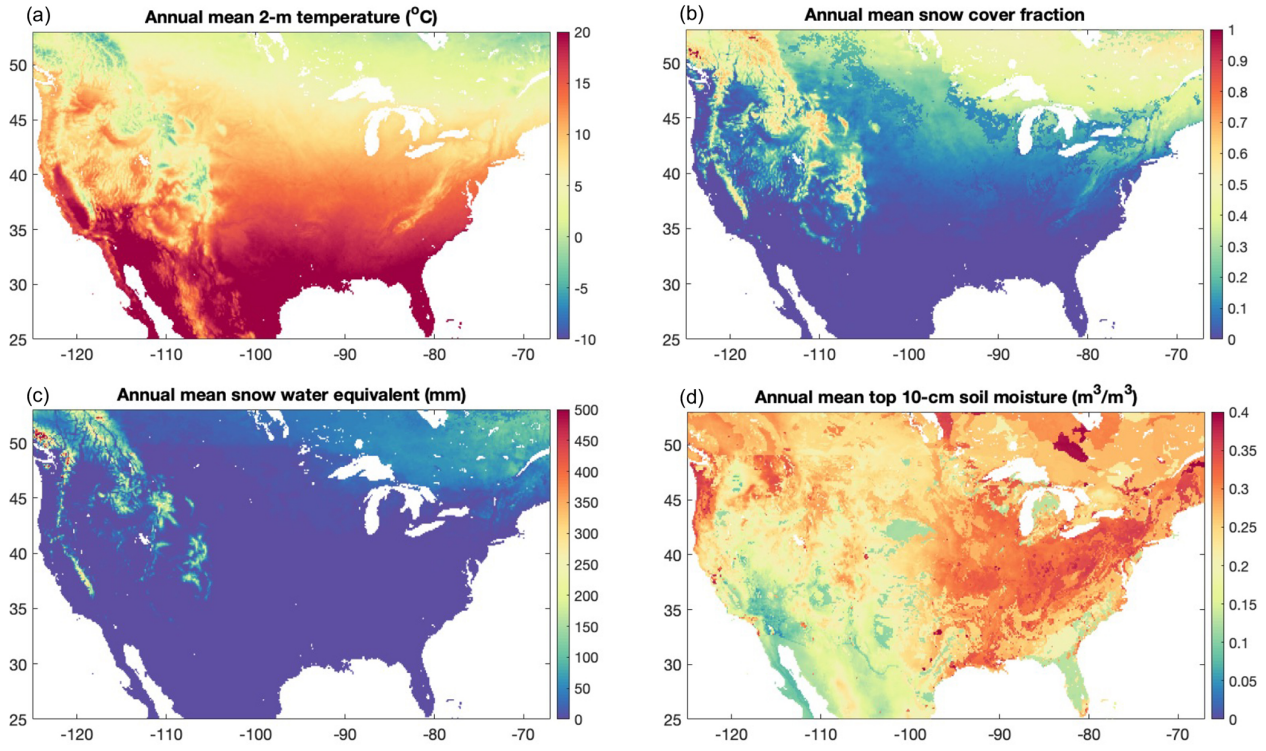

Figure 11. Demonstration of the 20-year (2001–2020) annual mean **(a)** 2 m temperature, **(b)** snow cover fraction, **(c)** snow water equivalent, and **(d)** top 10 cm soil moisture from the Noah-MP version 5.0 12 km continental US benchmark simulations driven by the NLDAS-2 atmospheric forcings.

the refactored and base simulations, with similar computational efficiency.

In addition, in order to provide the community with reference Noah-MP v5.0 model datasets for future comparison and assessment, we have conducted three sets of benchmark simulations, including 21-year (2000–2020) 12 km continental US simulations driven by the NLDAS-2 atmospheric forcings (Xia et al., 2012); 10-year (2009–2018) point-scale SNOTEL site 804 simulations over the western US, driven by observed precipitation and temperature, as well as other NLDAS-2 atmospheric forcings downscaled to 90 m spatial resolution (He et al., 2021); and 1-year (2000) 4 km dynamic crop simulations over the US Corn Belt region, driven by the convection-permitting WRF modeling (Zhang et al., 2020). We have archived all the atmospheric forcing datasets, model setup input datasets, and model output datasets for these benchmark simulations. Figure 11 shows an example of the model output. Note that a comprehensive evaluation of the simulation results is outside the scope of this model description paper and will be done in the next step.

9 Model code and technical documentation for Noah-MP version 5.0

We archive, manage, and maintain the Noah-MP v5.0 (together with previous code versions) at the NCAR community Noah-MP GitHub repository (https://github.com/NCAR/noahmp) for public access. We have also created a comprehensive technical documentation (He et al., 2023a) for the Noah-MP v5.0, available at https://doi.org/10.5065/ew8g-yr95, which provides detailed descriptions of model physics and formulations.

10 Conclusions and future plans

In this study, we modernized the widely used state-of-the-art Noah-MP LSM by adopting modern Fortran 2003 code standards and data structures, which substantially enhance the model modularity, interoperability, and applicability. The modernized Noah-MP has been released as the model version 5.0, which includes the following key features: (1) enhanced modularization as a result of re-organizing the model physics into individual process-level Fortran module files, (2) an enhanced data structure with new hierarchical data types and optimized variable declaration and initialization structures, (3) an enhanced code structure and calling workflow as a re-

sult of leveraging the new data structure and modularization, (4) an enhanced (descriptive and self-explanatory) model variable naming standard, and (5) an enhanced driver and interface structure to couple with host weather, climate, and hydrology models. The base code used for modernization is the Noah-MP version 4.5 (released in December 2022), and the modernization effort does not change the model physics. In addition, we have created a comprehensive technical documentation (He et al., 2023a) of the Noah-MP v5.0 and a set of benchmark simulation datasets.

The Noah-MP v5.0 has been recently coupled to the NCAR/HRLDAS system and the Korean Integrated Model (KIM) system. Currently, the work of coupling the Noah-MP v5.0 with the latest NASA/LIS system and the WRF-Hydro/NWM system is ongoing. The future plans for Noah-MP developments and applications include but are not limited to (1) coupling it with other widely used weather and climate models (e.g., WRF, MPAS, NOAA/UFS); (2) enhancing the capability of land data assimilation with Noah-MP; (3) enhancing plant hydraulics and soil hydraulics or hydrology schemes; (4) improving the accuracy of applications in subseasonal-to-seasonal (S2S) forecasts and forecasts of food–water security and extreme weather and climate (e.g., fire, drought, flood, and heat waves); (5) including automated model parameter calibration and optimization algorithms; (6) enhancing modeling capabilities for rapid landscape transformation (e.g., deforestation or reforestation), as well as for vegetation recovery and replacement after environmental disturbance; (7) including human management modeling (e.g., groundwater pumping); (8) including interactions with air pollution (e.g., pollutants' deposition and ozone damage to vegetation); (9) enhancing the representation of subgrid heterogeneity; (10) improving high-resolution input datasets (e.g., soil properties and groundwater-related inputs); and (11) creating a set of packages for code benchmarking and testing, model diagnostics, and better debugging capability. Overall, the modernized open-source community Noah-MP model allows for a more efficient and convenient process for future model developments and applications.

Code and data availability.

1. The Noah-MP model code (https://doi.org/10.5281/zenodo.7901855, He et al., 2023b) is available at https://github.com/NCAR/noahmp (last access: 4 September 2023).
2. The coupled HRLDAS/Noah-MP model code (https://doi.org/10.5281/zenodo.7901867, He et al., 2023c) is available at https://github.com/NCAR/hrldas.
3. The Noah-MP technical documentation is available at https://doi.org/10.5065/ew8g-yr95 (He et al., 2023a).
4. The benchmark datasets are stored in the NCAR high-performance supercomputer (HPC) campaign storage file system (data path: /glade/campaign/ral/hap/cenlinhe/NoahMP_benchmark/; see details about the storage system at https://arc.ucar.edu/knowledge_base/70549621, Smith, 2023) and can be provided by the corresponding author upon request due to the extremely large data size (8.8 TB).

Author contributions. CH, PV, and MB led the code-refactoring effort with the help of all the other co-authors (FC, DG, RC, GN, ZLY, DN, ME, TS, and RR). CH and PV led the technical-documentation-writing effort with the help of all the other co-authors (MB, FC, DG, RC, GN, ZLY, DN, ME, TS, and RR). CH conducted the benchmark model simulations. CH drafted the paper, with improvements made by all the other co-authors (PV, FC, MB, DG, RC, GN, ZLY, DN, ME, TS, and RR).

Competing interests. The contact author has declared that none of the authors has any competing interests.

Disclaimer. Publisher's note: Copernicus Publications remains neutral with regard to jurisdictional claims in published maps and institutional affiliations.

Acknowledgements. The authors thank the two reviewers for their constructive comments. We also thank Zhe Zhang (NCAR) and Ronnie Abolafia-Rosenzweig (NCAR) for helping with the model code testing and for the helpful discussions. Furthermore, we are grateful for the strong support from the entire Noah-MP community. Prasanth Valayamkunnath acknowledges the Department of Science and Technology, India, for the INSPIRE Faculty Fellowship (faculty registration no. IFA21-EAS 90). This study was supported by the US Geological Survey (USGS) Water Mission Area's Integrated Water Prediction program (grant no. 140G0121F0357, award ID no. 001548-00007); NOAA's Climate Program Office's Modeling, Analysis, Predictions, and Projections (MAPP) program (grant no. NA20OAR4310421); and the NCAR Water System Program. The National Center for Atmospheric Research (NCAR) is a major facility sponsored by the National Science Foundation (NSF) under the cooperative agreement no. 1852977. Any opinions, findings, conclusions, or recommendations expressed in this publication are those of the authors and do not necessarily reflect the views of the National Science Foundation.

Financial support. This study was supported by the US Geological Survey (USGS) Water Mission Area's Integrated Water Prediction program (grant no. 140G0121F0357, award ID no. 001548-00007).

Review statement. This paper was edited by Jatin Kala and reviewed by two anonymous referees.

References

Abolafia-Rosenzweig, R., He, C., Burns, S. P., and Chen, F.: Implementation and Evaluation of a Unified Turbulence Pa-

rameterization Throughout the Canopy and Roughness Sublayer in Noah-MP Snow Simulations, J. Adv. Model Earth Sy., 13, e2021MS002665, https://doi.org/10.1029/2021MS002665, 2021.

Abolafia-Rosenzweig, R., He, C., and Chen, F.: Winter and spring climate explains a large portion of interannual variability and trend in western U.S. summer fire burned area, Environ. Res. Lett., 17, 054030, https://doi.org/10.1088/1748-9326/ac6886, 2022a.

Abolafia-Rosenzweig, R., He, C., McKenzie Skiles, S., Chen, F., and Gochis, D.: Evaluation and Optimization of Snow Albedo Scheme in Noah-MP Land Surface Model Using In Situ Spectral Observations in the Colorado Rockies, J. Adv. Model Earth Sy., 14, e2022MS003141m https://doi.org/10.1029/2022MS003141, 2022b.

Abolafia-Rosenzweig, R., He, C., Chen, F., Ikeda, K., Schneider, T., and Rasmussen, R.: High resolution forecasting of summer drought in the western United States, Water Resour. Res., 59, e2022WR033734, https://doi.org/10.1029/2022WR033734, 2023a.

Abolafia-Rosenzweig, R., He, C., Chen, F., Zhang, Y., Dugger, A., Livneh, B., and Gochis, D.: Evaluating Noah-MP simulated runoff and snowpack in heavily burned Pacific-Northwest snow-dominated catchments, J. Geophys. Res.-Atmos., in review, 2023b.

Anderson, E. A.: A point energy and mass balance model of a snow cover, NOAA Tech. Rep. NWS 19, Off. of Hydrol., Natl. Weather Serv., Silver Spring, Md., 150 pp., https://repository.library.noaa.gov/view/noaa/6392 (last access: 4 September 2023), 1976.

Arsenault, K. R., Shukla, S., Hazra, A., Getirana, A., McNally, A., Kumar, S. V., Koster, R. D., Peters-Lidard, C. D., Zaitchik, B. F., Badr, H., Jung, H. C., Narapusetty, B., Navari, M., Wang, S., Mocko, D. M., Funk, C., Harrison, L., Husak, G. J., Adoum, A., Galu, G., Magadzire, T., Roningen, J., Shaw, M., Eylander, J., Bergaoui, K., McDonnell, R. A., and Verdin, J. P.: Better Advance Warnings of Drought, B. Am. Meteorol. Soc., 101, 899–903, 2020.

Ball, J. T., Woodrow, I. E., and Berry, J. A.: A model predicting stomatal conductance and its contribution to the control of photosynthesis under different environmental conditions, in: Process in Photosyn. Res., Vol. 1, edited by: Biggins, J., Martinus Nijhoff, Dordrecht, Netherlands, 221–234, 1987.

Barlage, M., Tewari, M., Chen, F., Miguez-Macho, G., Yang, Z. L., and Niu, G. Y.: The effect of groundwater interaction in North American regional climate simulations with WRF/Noah-MP, Climatic Change, 129, 485–498, https://doi.org/10.1007/s10584-014-1308-8, 2015.

Barlage, M., Chen, F., Rasmussen, R., Zhang, Z., and Miguez-Macho, G.: The importance of scale-dependent groundwater processes in land-atmosphere interactions over the central United States, Geophys. Res. Lett., 48, e2020GL092171, https://doi.org/10.1029/2020GL092171, 2021.

Blyth, E. M., Arora, V. K., Clark, D. B., Dadson, S. J., De Kauwe, M. G., Lawrence, D. M., Melton, J. R., Pongratz, J., Turton, R. H., Yoshimura, K., and Yuan, H.: Advances in land surface modelling, Curr. Clim. Change Rep., 7, 45–71, https://doi.org/10.1007/s40641-021-00171-5, 2021.

Bonan, G. B.: A land surface model (LSM version 1.0) for ecological, hydrological, and atmospheric studies: Technical description and user's guide, NCAR Tech. Note, NCAR/TN-417+STR, Natl. Cent. for Atmos. Res., Boulder, Colorado, 150 pp., https://doi.org/10.5065/D6DF6P5X, 1996.

Bonan, G. B. and Doney, S. C.: Climate, ecosystems, and planetary futures: The challenge to predict life in Earth system models, Science, 359, eaam8328, https://doi.org/10.1126/science.aam8328, 2018.

Brunsell, N. A., de Oliveira, G., Barlage, M., Shimabukuro, Y., Moraes, E., and Aragao, L.: Examination of seasonal water and carbon dynamics in eastern Amazonia: a comparison of Noah-MP and MODIS, Theor. Appl. Climatol., 143, 571–586, https://doi.org/10.1007/s00704-020-03435-6, 2021.

Brutsaert, W.: Evaporation into the Atmosphere: Theory, History, and Applications, Springer, Dordrecht, https://doi.org/10.1007/978-94-017-1497-6, 1982.

Cai, X., Yang, Z. L., David, C. H., Niu, G. Y., and Rodell, M.: Hydrological evaluation of the Noah-MP land surface model for the Mississippi River Basin, J. Geophys. Res.-Atmos., 119, 23–38, https://doi.org/10.1002/2013JD020792, 2014.

Cai, X., Yang, Z.-L., Fisher, J. B., Zhang, X., Barlage, M., and Chen, F.: Integration of nitrogen dynamics into the Noah-MP land surface model v1.1 for climate and environmental predictions, Geosci. Model Dev., 9, 1–15, https://doi.org/10.5194/gmd-9-1-2016, 2016.

Chang, M., Cao, J., Zhang, Q., Chen, W., Wu, G., Wu, L., Wang, W., and Wang, X.: Improvement of stomatal resistance and photosynthesis mechanism of Noah-MP-WDDM (v1.42) in simulation of NO_2 dry deposition velocity in forests, Geosci. Model Dev., 15, 787–801, https://doi.org/10.5194/gmd-15-787-2022, 2022.

Chen, F. and Dudhia, J.: Coupling an advanced land surface–hydrology model with the Penn State–NCAR MM5 Modeling System. Part I: Model implementation and sensitivity, Mon. Weather Rev., 129, 17, https://doi.org/10.1175/1520-0493(2001)129<0569:caalsh>2.0.co;2, 2001.

Chen, F. and Zhang, Y.: On the coupling strength between the land surface and the atmosphere: From viewpoint of surface exchange coefficients, Geophys. Res. Lett., 36, L10404, https://doi.org/10.1029/2009GL037980, 2009.

Chen, F., Mitchell, K., Schaake, J., Xue, Y., Pan, H. L., Koren, V., Duan, Q. Y., Ek, M. and Betts, A.: Modeling of land surface evaporation by four schemes and comparison with FIFE observations, J. Geophys. Res.-Atmos., 101, 7251–7268, https://doi.org/10.1029/95JD02165, 1996.

Chen, F., Janjicì, Z., and Mitchell, K.: Impact of atmospheric surface-layer parameterizations in the new land-surface scheme of the NCEP Mesoscale Eta Model, Bound.-Lay. Meteorol., 85, 391–421, https://doi.org/10.1023/A:1000531001463, 1997.

Chen, L., Li, Y., Chen, F., Barr, A., Barlage, M., and Wan, B.: The incorporation of an organic soil layer in the Noah-MP land surface model and its evaluation over a boreal aspen forest, Atmos. Chem. Phys., 16, 8375–8387, https://doi.org/10.5194/acp-16-8375-2016, 2016.

Dickinson, R. E.: Land surface processes and climate-surface albedos and energy balance, in: Adv. Geophys., vol. 25, edited by: Saltzman, B., Academic, San Diego, Calif., 305–353, https://doi.org/10.1016/S0065-2687(08)60176-4, 1983.

Dickinson, R. E., Henderson-Sellers, A., and Kennedy, P. J.: Biosphere-Atmosphere Transfer Scheme (BATS) version 1e as coupled to the NCAR Community Climate Model, NCAR Tech.

Note, NCAR/TN- 387+STR, 80 pp., Natl. Cent. for Atmos. Res., Boulder, Colo., https://doi.org/10.5065/D67W6959, 1993.

Dickinson, R. E., Shaikh, M., Bryant, R., and Graumlich, L.: Interactive canopies for a climate model, J. Climate, 11, 2823–2836, https://doi.org/10.1175/1520-0442(1998)011<2823:ICFACM>2.0.CO;2, 1998.

Ek, M. B., Mitchell, K. E., Lin, Y., Rogers, E., Grunmann, P., Koren, V., Gayno, G. and Tarpley, J. D.: Implementation of Noah land surface model advances in the National Centers for Environmental Prediction operational mesoscale Eta model, J. Geophys. Res.-Atmos., 108, 8851, https://doi.org/10.1029/2002JD003296, 2003.

Fan, Y., Miguez-Macho, G., Weaver, C. P., Walko, R., and Robock, A.: Incorporating water table dynamics in climate modeling: 1. Water table observations and equilibrium water table simulations, J. Geophys. Res.-Atmos., 112, D10125, https://doi.org/10.1029/2006JD008111, 2007.

Gao, Y., Xiao, L., Chen, D., Chen, F., Xu, J., and Xu, Y.: Quantification of the relative role of land-surface processes and large-scale forcing in dynamic downscaling over the Tibetan Plateau, Clim. Dynam., 48, 1705–1721, https://doi.org/10.1007/s00382-016-3168-6, 2017.

Hazra, A., McNally, A., Slinski, K., Arsenault, K. R., Shukla, S., Getirana, A., Jacob, J. P., Sarmiento, D. P., Peters-Lidard, C., Kumar, S. V., and Koster, R. D.: NASA's NMME-based S2S hydrologic forecast system for food insecurity early warning in southern Africa, J. Hydrol., 617, 129005, https://doi.org/10.1016/j.jhydrol.2022.129005, 2023.

He, C., Chen, F., Barlage, M., Liu, C., Newman, A., Tang, W., Ikeda, K., and Rasmussen, R.: Can convection-permitting modeling provide decent precipitation for offline high-resolution snowpack simulations over mountains, J. Geophys. Res.-Atmos., 124, 12631–12654, https://doi.org/10.1029/2019JD030823, 2019.

He, C., Chen, F., Abolafia-Rosenzweig, R., Ikeda, K., Liu, C. and Rasmussen, R.: What causes the unobserved early-spring snowpack ablation in convection-permitting WRF modeling over Utah mountains?, J. Geophys. Res.-Atmos, 126, e2021JD035284, https://doi.org/10.1029/2021JD035284, 2021.

He, C., Valayamkunnath, P., Barlage, M., Chen, F., Gochis, D., Cabell, R., Schneider, T., Rasmussen, R., Niu, G. Y., Yang, Z. L., Niyogi, D., and Ek, M.: The Community Noah-MP Land Surface Modeling System Technical Description Version 5.0, NCAR Tech. Note, No. NCAR/TN-575+STR, https://doi.org/10.5065/ew8g-yr95, 2023a.

He, C., Barlage, M., Valayamkunnath, P., Gill, D., Mocko, D., and Chen. F.: NCAR/noahmp: Release of v5.0.0 (v5.0.0), Zenodo [code]. https://doi.org/10.5281/zenodo.7901855, 2023b.

He, C., Barlage, M., Zhang, Z., xutr-bnu, Mocko, D., and Chen, F.: NCAR/hrldas: Release of v5.0.0 (v5.0.0), Zenodo [code], https://doi.org/10.5281/zenodo.7901868, 2023c.

Ingwersen, J., Högy, P., Wizemann, H. D., Warrach-Sagi, K., and Streck, T.: Coupling the land surface model Noah-MP with the generic crop growth model Gecros: Model description, calibration and validation, Agr. Forest Meteorol., 262, 322–339, https://doi.org/10.1016/j.agrformet.2018.06.023, 2018.

Jarvis, P. G.: The interpretation of the variations in leaf water potential and stomatal conductance found in canopies in the field, Philos. T. R. Soc. B, 273, 593–610, https://doi.org/10.1098/rstb.1976.0035, 1976.

Jayawardena, A. W. and Zhou, M. C.: A modified spatial soil moisture storage capacity distribution curve for the Xinanjiang model, J. Hydrol., 227, 93–113, https://doi.org/10.1016/S0022-1694(99)00173-0, 2000.

Jiang, Y., Chen, F., Gao, Y., He, C., Barlage, M., and Huang, W.: Assessment of uncertainty sources in snow cover simulation in the Tibetan Plateau, J. Geophys. Res.-Atmos., 125, e2020JD032674, https://doi.org/10.1029/2020JD032674, 2020.

Jiang, Y., Gao, Y., He, C., Liu, B., Pan, Y., and Li, X.: Spatiotemporal distribution and variation of wind erosion over the Tibetan Plateau based on a coupled land-surface wind-erosion model, Aeolian Res., 50, 100699, https://doi.org/10.1016/j.aeolia.2021.100699, 2021.

Jordan, R.: A one-dimensional temperature model for a snow cover, Spec. Rep. 91–16, Cold Reg. Res. and Eng. Lab., U.S. Army Corps. of Eng., Hanover, N. H., 1991.

Ju, C., Li, H., Li, M., Liu, Z., Ma, Y., Mamtimin, A., Sun, M., and Song, Y.: Comparison of the Forecast Performance of WRF Using Noah and Noah-MP Land Surface Schemes in Central Asia Arid Region, Atmosphere, 13, 927, https://doi.org/10.3390/atmos13060927, 2022.

Koren, V., Schaake, J. C., Mitchell, K. E., Duan, Q.-Y., Chen, F., and Baker, J. M.: A parameterization of snowpack and frozen ground intended for NCEP weather and climate models, J. Geophys. Res., 104, 19569–19585, https://doi.org/10.1029/1999JD900232, 1999.

Kumar, S. V., Mocko, D. M., Wang, S., Peters-Lidard, C. D., and Borak, J.: Assimilation of remotely sensed leaf area index into the Noah-MP land surface model: Impacts on water and carbon fluxes and states over the continental United States, J. Hydrometeorol., 20, 1359–1377, 2019.

Kumar, S. V., Holmes, T., Andela, N., Dharssi, I., Vinodkumar, Hain, C., Peters-Lidard, C., Mahanama, S. P., Arsenault, K. R., Nie, W., and Getirana, A.: The 2019–2020 Australian drought and bushfires altered the partitioning of hydrological fluxes, Geophys. Res. Lett., 48, e2020GL091411, https://doi.org/10.1029/2020GL091411, 2021.

Li, J., Chen, F., Lu, X., Gong, W., Zhang, G., and Gan, Y.: Quantifying contributions of uncertainties in physical parameterization schemes and model parameters to overall errors in Noah-MP dynamic vegetation modeling, J. Adv. Model. Earth Sy., 12, e2019MS001914, https://doi.org/10.1029/2019MS001914, 2020.

Li, L., Yang, Z. L., Matheny, A. M., Zheng, H., Swenson, S. C., Lawrence, D. M., Barlage, M., Yan, B., McDowell, N. G., and Leung, L. R.: Representation of plant hydraulics in the Noah-MP land surface model: Model development and multi-scale evaluation, J. Adv. Model. Earth Sy., 13, e2020MS002214, https://doi.org/10.1029/2020MS002214, 2021.

Li, M., Wu, P., Ma, Z., Lv, M., Yang, Q., and Duan, Y.: The decline in the groundwater table depth over the past four decades in China simulated by the Noah-MP land model, J. Hydrol., 607, 127551, https://doi.org/10.1016/j.jhydrol.2022.127551, 2022.

Li, X., Wu, T., Zhu, X., Jiang, Y., Hu, G., Hao, J., Ni, J., Li, R., Qiao, Y., Yang, C., Ma, W., Wen, A., and Ying, X.: Improving the Noah-MP model for simulating hydrothermal regime of the active layer in the permafrost regions of the Qinghai-Tibet Plateau, J. Geophys. Res.-Atmos., 125, e2020JD032588, https://doi.org/10.1029/2020JD032588, 2020.

Liang, J., Yang, Z., and Lin, P.: Systematic hydrological evaluation of the Noah-MP land surface model over China, Adv. Atmos. Sci., 36, 1171–1187, https://doi.org/10.1007/s00376-019-9016-y, 2019.

Liang, X. and Xie, Z.: Important factors in land–atmosphere interactions: surface runoff generations and interactions between surface and groundwater, Global Planet. Change, 38, 101–114, https://doi.org/10.1016/S0921-8181(03)00012-2, 2003.

Liang, X., Lettenmaier, D. P., Wood, E. F., and Burges, S. J.: A simple hydrologically based model of land surface water and energy fluxes for general circulation models, J. Geophys. Res.-Atmos., 99, 14415–14428, https://doi.org/10.1029/94JD00483, 1994.

Liu, C., Ikeda, K., Rasmussen, R., Barlage, M., Newman, A. J., Prein, A. F., Chen, F., Chen, L., Clark, M., Dai, A., Dudhia, J., Eidhammer, T., Gochis, D., Gutmann, E., Kurkute, S., Li, Y., Thompson, G., and Yates, D.: Continental-scale convection-permitting modeling of the current and future climate of North America, Clim. Dynam., 49, 71–95, https://doi.org/10.1007/s00382-016-3327-9, 2017.

Liu, X., Chen, F., Barlage, M., Zhou, G., and Niyogi, D.: Noah-MP-Crop: Introducing dynamic crop growth in the Noah-MP land surface model, J. Geophys. Res.-Atmos., 121, 13953–13972, https://doi.org/10.1002/2016JD025597, 2016.

McDaniel, R., Liu, Y., Valayamkunnath, P., Barlage, M., Gochis, D., Cosgrove, B. A., and Flowers, T.: Moisture condition impact and seasonality of National Water Model performance under different runoff-infiltration partitioning schemes, in: AGU Fall Meeting Abstracts, Vol. 2020, 2020AGUFMH111.0028M, 2020.

Miguez-Macho, G., Fan, Y., Weaver, C. P., Walko, R., and Robock, A.: Incorporating water table dynamics in climate modeling: 2. Formulation, validation, and soil moisture simulation, J. Geophys. Res.-Atmos., 112, D13108, https://doi.org/10.1029/2006JD008112, 2007.

Nie, W., Kumar, S. V., Arsenault, K. R., Peters-Lidard, C. D., Mladenova, I. E., Bergaoui, K., Hazra, A., Zaitchik, B. F., Mahanama, S. P., McDonnell, R., Mocko, D. M., and Navari, M.: Towards effective drought monitoring in the Middle East and North Africa (MENA) region: implications from assimilating leaf area index and soil moisture into the Noah-MP land surface model for Morocco, Hydrol. Earth Syst. Sci., 26, 2365–2386, https://doi.org/10.5194/hess-26-2365-2022, 2022.

Niu, G.-Y. and Yang, Z.-L.: The effects of canopy processes on snow surface energy and mass balances, J. Geophys. Res.-Atmos., 109, D23111, https://doi.org/10.1029/2004JD004884, 2004.

Niu, G.-Y. and Yang, Z.-L.: Effects of frozen soil on snowmelt runoff and soil water storage at a continental scale, J. Hydrometeorol., 7, 937–952, https://doi.org/10.1175/JHM538.1, 2006.

Niu, G.-Y., Yang, Z.-L., Dickinson, R. E., and Gulden, L. E.: A simple TOPMODEL-based runoff parameterization (SIMTOP) for use in global climate models, J. Geophys. Res.-Atmos., 110, D21106, https://doi.org/10.1029/2005JD006111, 2005.

Niu, G.-Y., Yang, Z.-L., Dickinson, R. E., Gulden, L. E., and Su, H.: Development of a simple groundwater model for use in climate models and evaluation with Gravity Recovery and Climate Experiment data, J. Geophys. Res.-Atmos., 112, D07103, https://doi.org/10.1029/2006JD007522, 2007.

Niu, G. Y., Yang, Z. L., Mitchell, K. E., Chen, F., Ek, M. B., Barlage, M., Kumar, A., Manning, K., Niyogi, D., Rosero, E., Tewari, M., and Xia, Y.: The community Noah land surface model with multiparameterization options (Noah-MP): 1. Model description and evaluation with local-scale measurements, J. Geophys. Res.-Atmos., 116, D12109, https://doi.org/10.1029/2010JD015139, 2011.

Niu, G. Y., Fang, Y. H., Chang, L. L., Jin, J., Yuan, H., and Zeng, X.: Enhancing the Noah-MP ecosystem response to droughts with an explicit representation of plant water storage supplied by dynamic root water uptake, J. Adv. Model. Earth Sy., 12, e2020MS002062, https://doi.org/10.1029/2020MS002062, 2020.

Oleson, K., Dai, Y., Bonan, B., Bosilovichm, M., Dickinson, R., Dirmeyer, P., Hoffman, F., Houser, P., Levis, S., Niu, G. Y., Thornton, P., Vertenstein, M., Yang, Z. L., and Zeng, X.: Technical description of the Community Land Model (CLM), NCAR Tech. Note, NCAR/TN-461+STR, Natl. Cent. for Atmos. Res., Boulder, Colo., 174 pp., https://doi.org/10.5065/D6N877R0, 2004.

Patel, P., Jamshidi, S., Nadimpalli, R., Aliaga, D. G., Mills, G., Chen, F., Demuzere, M., and Niyogi, D.: Modeling Large-Scale Heatwave by Incorporating Enhanced Urban Representation, J. Geophys. Res.-Atmos., 127, e2021JD035316, https://doi.org/10.1029/2021JD035316, 2022.

Rasmussen, R., Chen, F., Liu, C., Ikeda, K., Prein, A., Kim, J.-H., Schneider, T., Dai, A., Gochis, D., Dugger, A., Zhang, Y., Jaye, A., Dudhia, J., He, C., Harrold, M., Xue, L., Chen, S., Newman, A., Dougherty, E., Abolafia-Rosenzweig, R., Lybarger, N., Viger, R., Lesmes, D. P., Skalak, K., Brakebill, J. W., Clline, D., Dunne, K., Rasmussen, K., and Miguez-Macho, G.: CONUS404: The NCAR-USGS 4-km long-term regional hydroclimate reanalysis over the CONUS, B. Am. Meteorol. Soc., E1382–E1408, https://doi.org/10.1175/BAMS-D-21-0326.1, 2023.

Sakaguchi, K. and Zeng, X.: Effects of soil wetness, plant litter, and under-canopy atmospheric stability on ground evaporation in the Community Land Model (CLM3. 5), J. Geophys. Res.-Atmos., 114, D01107, https://doi.org/10.1029/2008JD010834, 2009.

Salamanca, F., Zhang, Y., Barlage, M., Chen, F., Mahalov, A., and Miao, S.: Evaluation of the WRF-urban modeling system coupled to Noah and Noah-MP land surface models over a semiarid urban environment, J. Geophys. Res.-Atmos., 123, 2387–2408, https://doi.org/10.1002/2018JD028377, 2018.

Saxton, K. E. and Rawls, W. J.: Soil water characteristic estimates by texture and organic matter for hydrologic solutions, Soil Sci. Soc. Am. J., 70, 1569–1578, https://doi.org/10.2136/sssaj2005.0117, 2006.

Sellers, P. J.: Canopy reflectance, photosynthesis and transpiration, Int. J. Remote Sens., 6, 1335–1372, https://doi.org/10.1080/01431168508948283, 1985.

Sellers, P. J., Heiser, M. D., and Hall, F. G.: Relations between surface conductance and spectral vegetation indices at intermediate (100 m^2 to 15 km^2) length scales, J. Geophys. Res.-Atmos., 97, 19033–19059, https://doi.org/10.1029/92JD01096, 1992.

Schaake, J. C., Koren, V. I., Duan, Q. Y., Mitchell, K., and Chen, F.: Simple water balance model for estimating runoff at different spatial and temporal scales, J. Geophys. Res.-Atmos., 101, 7461–7475, https://doi.org/10.1029/95JD02892, 1996.

Shu, Z., Zhang, B., Tian, L., and Zhao, X.: Improving Dynamic Vegetation Modeling in Noah-MP by Parameter

Optimization and Data Assimilation Over China's Loess Plateau, J. Geophys. Res.-Atmos., 127, e2022JD036703, https://doi.org/10.1029/2022JD036703, 2022.

Smith, B. J.: Campaign Storage file system, https://arc.ucar.edu/knowledge_base/70549621 (last access: 4 September 2023), 2023.

Suzuki, K. and Zupanski, M.: Uncertainty in solid precipitation and snow depth prediction for Siberia using the Noah and Noah-MP land surface models, Front. Earth Sci., 12, 672–682, https://doi.org/10.1007/s11707-018-0691-2, 2018.

Valayamkunnath, P., Chen, F., Barlage, M. J., Gochis, D. J., Franz, K. J., and Cosgrove, B. A.: Impact of Agriculture Management Practices on the National Water Model Simulated Streamflow, in: 101st Am. Meteorol. Soc. Annual Meeting, https://ams.confex.com/ams/101ANNUAL/meetingapp.cgi/Paper/383317 (last access: 4 September 2023), 2021.

Valayamkunnath, P., Gochis, D. J., Chen, F., Barlage, M., and Franz, K. J.: Modeling the hydrologic influence of subsurface tile drainage using the National Water Model, Water Resour. Res., 58, e2021WR031242, https://doi.org/10.1029/2021WR031242, 2022.

Verseghy, D. L.: CLASS-A Canadian land surface scheme for GCMS: I. Soil model, Int. J. Climatol., 11, 111–133, https://doi.org/10.1002/joc.3370110202, 1991.

Wang, P., Niu, G. Y., Fang, Y. H., Wu, R. J., Yu, J. J., Yuan, G. F., Pozdniakov, S. P., and Scott, R. L.: Implementing dynamic root optimization in Noah-MP for simulating phreatophytic root water uptake, Water Resour. Res., 54, 1560–1575, https://doi.org/10.1002/2017WR021061, 2018.

Wang, W., Yang, K., Zhao, L., Zheng, Z., Lu, H., Mamtimin, A., Ding, B., Li, X., Zhao, L., Li, H., Che, T., and Moore, J. C.: Characterizing surface albedo of shallow fresh snow and its importance for snow ablation on the interior of the Tibetan Plateau, J. Hydrometeorol., 21, 815–827, https://doi.org/10.1175/JHM-D-19-0193.1, 2020.

Wang, W., He, C., Moore, J., Wang, G., and Niu, G. Y.: Physics-Based Narrowband Optical Parameters for Snow Albedo Simulation in Climate Models, J. Adv. Model. Earth Syst., 14, e2020MS002431, https://doi.org/10.1029/2020MS002431, 2022.

Wang, Y. H., Broxton, P., Fang, Y., Behrangi, A., Barlage, M., Zeng, X., and Niu, G. Y.: A wet-bulb temperature-based rain-snow partitioning scheme improves snowpack prediction over the drier western United States, Geophys. Res. Lett., 46, 13825–13835, https://doi.org/10.1029/2019GL085722, 2019.

Warrach-Sagi, K., Ingwersen, J., Schwitalla, T., Troost, C., Aurbacher, J., Jach, L., Berger, T., Streck, T., and Wulfmeyer, V.: Noah-MP with the generic crop growth model Gecros in the WRF model: Effects of dynamic crop growth on land-atmosphere interaction, J. Geophys. Res.-Atmos., 127, e2022JD036518, https://doi.org/10.1029/2022JD036518, 2022.

Wrzesien, M. L., Pavelsky, T. M., Kapnick, S. B., Durand, M. T., and Painter, T. H.: Evaluation of snow cover fraction for regional climate simulations in the Sierra Nevada, Int. J. Climatol., 35, 2472–2484, https://doi.org/10.1002/joc.4136, 2015.

Wu, W. Y., Yang, Z. L., and Barlage, M.: The Impact of Noah-MP Physical Parameterizations on Modeling Water Availability during Droughts in the Texas–Gulf Region, J. Hydrometeorol., 22, 1221–1233, https://doi.org/10.1175/JHM-D-20-0189.1, 2021.

Xia, Y., Mitchell, K., Ek, M., Sheffield, J., Cosgrove, B., Wood, E., Luo, L., Alonge, C., Wei, H., Meng, J., Livneh, B., Lettenmaier, D., Koren, V., Duan, Q., Mo, K., Fan, Y., and Mocko, D.: Continental-scale water and energy flux analysis and validation for the North American Land Data Assimilation System project phase 2 (NLDAS-2): 1. Intercomparison and application of model products, J. Geophys. Res.-Atmos., 117, D03109, https://doi.org/10.1029/2011JD016048, 2012.

Xu, T., Chen, F., He, X., Barlage, M., Zhang, Z., Liu, S., and He, X.: Improve the performance of the noah-MP-crop model by jointly assimilating soil moisture and vegetation phenology data, J. Adv. Model. Earth Sy., 13, e2020MS002394, https://doi.org/10.1029/2020MS002394, 2021.

Xu, X., Chen, F., Shen, S., Miao, S., Barlage, M., Guo, W., and Mahalov, A.: Using WRF-urban to assess summertime air conditioning electric loads and their impacts on urban weather in Beijing, J. Geophys. Res.-Atmos., 123, 2475–2490, https://doi.org/10.1002/ 2017JD028168, 2018.

Xue, Y., Sellers, P. J., Kinter, J. L., and Shukla, J.: A simplified biosphere model for global climate studies, J. Climate, 4, 345–364, https://doi.org/10.1175/1520-0442(1991)004<0345:ASBMFG>2.0.CO;2, 1991.

Yang, Z.-L. and Dickinson, R. E.: Description of the Biosphere-Atmosphere Transfer Scheme (BATS) for the soil moisture workshop and evaluation of its performance, Global Planet. Change, 13, 117–134, https://doi.org/10.1016/0921-8181(95)00041-0, 1996.

Yang, Z. L., Niu, G. Y., Mitchell, K. E., Chen, F., Ek, M. B., Barlage, M., Longuevergne, L., Manning, K., Niyogi, D., Tewari, M., and Xia, Y.: The community Noah land surface model with multiparameterization options (Noah-MP): 2. Evaluation over global river basins, J. Geophys. Res.-Atmos., 116, D12110, https://doi.org/10.1029/2010JD015140, 2011.

Yen, Y. C.: Effective thermal conductivity and water vapor diffusivity of naturally compacted snow, J. Geophys. Res.-Atmos., 70, 1821–1825, https://doi.org/10.1029/JZ070i008p01821, 1965.

Yen, Y. C.: Review of thermal properties of snow, ice, and sea ice, Vol. 81, No. 10, US Army Corps of Engineers, Cold Regions Research and Engineering Laboratory, 1981.

Zhang, G., Chen, F., and Gan, Y.: Assessing uncertainties in the Noah-MP ensemble simulations of a cropland site during the Tibet Joint International Cooperation program field campaign, J. Geophys. Res.-Atmos., 121, 9576–9596, https://doi.org/10.1002/2016JD024928, 2016.

Zhang, X., Xie, Z., Ma, Z., Barron-Gafford, G. A., Scott, R. L., and Niu, G. Y.: A Microbial-Explicit Soil Organic Carbon Decomposition Model (MESDM): Development and Testing at a Semiarid Grassland Site, J. Adv. Model. Earth Sy., 14, e2021MS002485, https://doi.org/10.1029/2021MS002485, 2022.

Zhang, X. Y., Jin, J., Zeng, X., Hawkins, C. P., Neto, A. A., and Niu, G. Y.: The compensatory CO_2 fertilization and stomatal closure effects on runoff projection from 2016–2099 in the western United States, Water Resour. Res., 58, e2021WR030046, https://doi.org/10.1029/2021WR030046, 2022.

Zhang, Z., Barlage, M., Chen, F., Li, Y., Helgason, W., Xu, X., Liu, X., and Li, Z.: Joint modeling of crop and irrigation in the central United States using the Noah-MP land surface model, J. Adv. Model. Earth Sy., 12, e2020MS002159, https://doi.org/10.1029/2020MS002159, 2020.

Zhang, Z., Chen, F., Barlage, M., Bortolotti, L. E., Famiglietti, J., Li, Z., Ma, X. and Li, Y.: Cooling Effects Revealed by Modeling of Wetlands and Land-Atmosphere Interactions, Water Resour. Res., 58, e2021WR030573, https://doi.org/10.1029/2021WR030573, 2022.

Zhang, Z., Li, Y., Chen, F., Harder, P., Helgason, W., Famiglietti, J., Valayamkunnath, P., He, C., and Li, Z.: Developing spring wheat in the Noah-MP land surface model (v4.4) for growing season dynamics and responses to temperature stress , Geosci. Model Dev., 16, 3809–3825, https://doi.org/10.5194/gmd-16-3809-2023, 2023.

Zhuo, L., Dai, Q., Han, D., Chen, N., and Zhao, B.: Assessment of simulated soil moisture from WRF Noah, Noah-MP, and CLM land surface schemes for landslide hazard application, Hydrol. Earth Syst. Sci., 23, 4199–4218, https://doi.org/10.5194/hess-23-4199-2019, 2019.

Zonato, A., Martilli, A., Gutierrez, E., Chen, F., He, C., Barlage, M., Zardi, D., and Giovannini, L.: Exploring the effects of rooftop mitigation strategies on urban temperatures and energy consumption, J. Geophys. Res.-Atmos., 126, e2021JD035002, https://doi.org/10.1029/2021JD035002, 2021.